Statistical Properties of NLIN in Presence of PDL

Ori Golani[1] and David Dahan[2,3]
[1]School of Electrical Engineering, Tel Aviv University, Tel Aviv, 69978, Israel
[2]Toga Networks, a Huawei company, 4 Haharash street, Hod Hasharon, 45240, Israel
[3]Department of Electrical Engineering, Holon Institute of Technology, 52 Golomb street, Holon, 58102, Israel
david.dahan@huawei.com

Abstract: We present an analytical model which predicts the statistical properties of nonlinear interference noise in fiber links affected by PDL. We show that many features of NLIN, such as its phase and polarization rotation noise may be significantly modified by PDL components present in the link.
OCIS codes: (060.2330) Fiber optics communications, (060.4370) Nonlinear Optics

1. Introduction

Simulations of large channel-count transmission systems are extremely demanding in term of computational resources and require unacceptably long computation time when relying on the conventional split-step Fourier-transform method (SSFTM), especially in wideband DWDM scenarios. Several models have been developed to capture the statistical behavior of the nonlinear interference noise (NLIN). The enhanced Gaussian noise (EGN) model predicts the variance of NLIN and adds it to the transmitted signal as a white Gaussian noise [1]. Alternatively, the XPM induced NLIN can be approximated as a time-varying inter-symbol interference (ISI) process with accurate estimations of its second order statistics [2-3]. This allows to precisely predict the properties of nonlinear phase and polarization rotation noise (PPRN) [4], as well as to design equalization-based methods of mitigating NLIN [5-6]. There is an ongoing effort of incorporating more and more physical effects into these models, making them more accurate. Recently, we introduced the Universal Virtual Lab, a simulation tool that allows a fast and accurate link performance assessment by generating the XPM induced NLIN as a time varying ISI process while accounting for practical system impairments such as inter-channel stimulated Raman scattering, transmitter IQ imbalance and WSS filters [6]. In addition, Serena et al. [7] have incorporated the effect of polarization dependent loss (PDL) into the EGN model in order to estimate the NLIN variance. Here, we model and investigate the statistical properties of the time-varying ISI model of XPM induced NLIN affected by PDL along the fiber link. We validate the analytical model by comparing to SSFM simulations.

2. Analytical model derivation

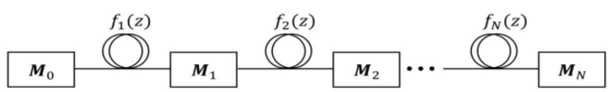

Fig. 1. Schematic layout of a fiber link, composed of fiber with no PDL and discrete PDL elements (described by PDL matrices $\mathbf{M}_k$ $0 \le k \le N$)

We consider two channels, A and B, spaced by angular frequency Ω, which are launched into the optical fiber link. We use the bra-ket notation as in [3] for a 2-element complex vector representing a dual polarization signal or symbol and matrices are denoted by boldface letters. The total electric field at point z, in the absence of nonlinearity but affected by fiber loss, chromatic dispersion and PDL is given by

$$|\mathrm{E}(t,z)\rangle = \sum_n \mathbf{U}(z)\, g(t-nT,z)|a_n\rangle + e^{-i\Omega t}\sum_{n'} \mathbf{U}(z)\, g(t-n'T,z)\mathbf{h}|b_{n'}\rangle \qquad (1)$$

Here, $g(t,z)$ describes the pulse shape at point z along the link, $|a_n\rangle$ and $|b_n\rangle$ are the n-th symbols of channel A and B, respectively and $\mathbf{U}(z)$ is a 2x2 matrix representing the gain/loss accumulated up to point z. Note that $\mathbf{U}(z)$ includes both the losses of the fiber itself and those of PDL-inducing components along the link. $\mathbf{h}$ is a 2x2 unitary rotation matrix representing the input state of polarization (SOP) of channel B, with respect to the orientation of channel A. It should be noted that the definition of $\mathbf{U}(z)$ implicitly assumes that no PMD is present in the link. This assumption can be removed by considering different gain/loss matrices for each interfering channel. However, this makes the derivation rather involved, and is not treated in this paper. In this development, we only consider discrete PDL elements along the link such as ROADMs and optical amplifiers as illustrated in Fig 1, allowing a decoupling between the effects induced by the fiber and the PDL elements. Within the first order perturbation theory, after applying zero-forcing equalization for compensation of the linear transmission impairments, the XPM induced nonlinear contribution of channel B affecting channel A is expressed in the same a manner as the time-varying ISI model developed in [3]

$$|\Delta a_n\rangle = \sum_l \mathbf{R}_l^{(n)}\, |a_{l+n}\rangle \qquad (2) \qquad \text{with} \qquad \mathbf{R}_l^{(n)} = \sum_{h,k} \left\langle b_k \middle| \mathbf{h}^\dagger \mathbf{W}_{h,k,l+n}^{(n)} \mathbf{h} \middle| b_h \right\rangle \mathbb{I}_2 + \mathbf{h}|b_h\rangle\langle b_k|\mathbf{h}^\dagger \mathbf{W}_{h,k,l+n}^{(n)} \qquad (3)$$

$$\mathbf{W}_{h,k,l+n}^{(n)} = \sum_p \boldsymbol{U}_p^\dagger \boldsymbol{U}_p I_{h,k,l,p}^{(n)} \ (4) \ \text{with} \ I_{h,k,l,p}^{(n)} = i\frac{8}{9}\gamma \int_{z_{p-1}}^{z_p}\int_{-\infty}^{\infty} g^*(t-nT,z)g(t-(l+n)T,z)g^*(t-kT-\beta_2\Omega z,z) \times g(t-hT-\beta_2\Omega z,z) f_{p-1}(z)\, dt\, dz \qquad (5)$$

Here, $\mathbb{I}_2$ is the 2x2 identity matrix, β_2 is the dispersion coefficient, $f_p(z)$ is the gain/loss profile of link segment p without the PDL components and the total accumulated PDL matrix up to point z_p, after p PDL elements is given by

$$\mathbf{U}_p = \mathbf{M}_{p-1}\mathbf{M}_{p-2}\cdots\mathbf{M}_0 \qquad (6)$$

3. Autocorrelations and cross-correlations of the ISI components

In order to derive the second-order statistics of the ISI matrices, we arrange the components of $\boldsymbol{R}_l^{(n)}$ in vector form: $\underline{R}_l^{(n)} = \left[R_{xx}^{(n)}, R_{xy}^{(n)}, R_{yx}^{(n)}, R_{yy}^{(n)}\right]^T$. Assuming a symmetric complex constellation, with i.i.d. symbols in both polarizations, the cross-correlation matrix of two such vectors is

$$\boldsymbol{C}_{l,l'}^{(\Delta n)} = \boldsymbol{Cov}\left[\underline{R}_l^{(0)}, \underline{R}_{l'}^{(\Delta n)}\right] = P^2\left(\mathbf{S}_{1,l,l'}^{(\Delta n)} + (M-2)\mathbf{S}_{2,l,l'}^{(\Delta n)}\right) \qquad (7)$$

where P is the power per polarization and $M = \mathbb{E}[b^4]/\mathbb{E}[b^2]^2$ is the normalized kurtosis,

$$\mathbf{S}_{1,l,l'}^{(\Delta n)} = \sum_{p,p'} \mathbf{V}_p \mathbf{H}\mathbf{H}^\dagger \mathbf{V}_{p'}^\dagger \underbrace{\sum_{h,k} I_{h,k,l,p}^{(0)} I_{h,k,l',p'}^{(\Delta n)*}}_{s_{1,l,l',p,p'}^{(\Delta n)}} \qquad (8) \qquad \mathbf{S}_{2,l,l'}^{(\Delta n)} = \sum_{p,p'} \mathbf{V}_p \mathbf{H} \begin{pmatrix} 1 & & & \\ & 0 & & \\ & & 0 & \\ & & & 1 \end{pmatrix} \mathbf{H}^\dagger \mathbf{V}_{p'}^\dagger \underbrace{\sum_{h} I_{h,h,l,p}^{(0)} I_{h,h,l',p'}^{(\Delta n)*}}_{s_{2,l,l',p,p'}^{(\Delta n)}} \qquad (9)$$

$$\mathbf{V}_p = \begin{pmatrix} 2(\mathbf{U}_p^\dagger\mathbf{U}_p)_{xx} & 2(\mathbf{U}_p^\dagger\mathbf{U}_p)_{yx} & (\mathbf{U}_p^\dagger\mathbf{U}_p)_{xy} & (\mathbf{U}_p^\dagger\mathbf{U}_p)_{yy} \\ (\mathbf{U}_p^\dagger\mathbf{U}_p)_{xy} & (\mathbf{U}_p^\dagger\mathbf{U}_p)_{yy} & 0 & 0 \\ 0 & 0 & (\mathbf{U}_p^\dagger\mathbf{U}_p)_{xx} & (\mathbf{U}_p^\dagger\mathbf{U}_p)_{yx} \\ (\mathbf{U}_p^\dagger\mathbf{U}_p)_{xx} & (\mathbf{U}_p^\dagger\mathbf{U}_p)_{yx} & 2(\mathbf{U}_p^\dagger\mathbf{U}_p)_{xy} & 2(\mathbf{U}_p^\dagger\mathbf{U}_p)_{yy} \end{pmatrix}, (10) \quad \mathbf{H} = \begin{pmatrix} |h_{xx}|^2 & h_{xx}h_{xy}^* & h_{xy}h_{xx}^* & |h_{xy}|^2 \\ h_{xx}h_{xy}^* & h_{xx}h_{yy}^* & h_{xy}h_{yx}^* & h_{xy}h_{yy}^* \\ h_{yx}h_{xx}^* & h_{yx}h_{xy}^* & h_{yy}h_{xx}^* & h_{yy}h_{xy}^* \\ |h_{yx}|^2 & h_{yx}h_{yy}^* & h_{yy}h_{yx}^* & |h_{yy}|^2 \end{pmatrix}, (11)$$

The main advantage of these results is that they allow to separate the effects of the fibers from those of discrete PDL components. The set of scalar coefficients $s_{1,l,l',p,p'}^{(\Delta n)}$ and $s_{2,l,l',p,p'}^{(\Delta n)}$ in Eqs (8-9) are independent of the PDL vectors of the link and the SOP, whereas the set of matrices $\mathbf{V}_p$ is extracted from the PDL vectors of discrete components along the link, and is independent of the fiber parameters and signal properties. While the numerical integration of the scalar coefficients requires computationally extensive numerical integration, determining the values of $\mathbf{H}$ for a given SOP and $\mathbf{V}_p$ for a given set of PDL vectors is done analytically and with practically negligible computation time. This means that many different PDL settings may be explored, without any significant additional computation cost.

4. Numerical validation and discussion

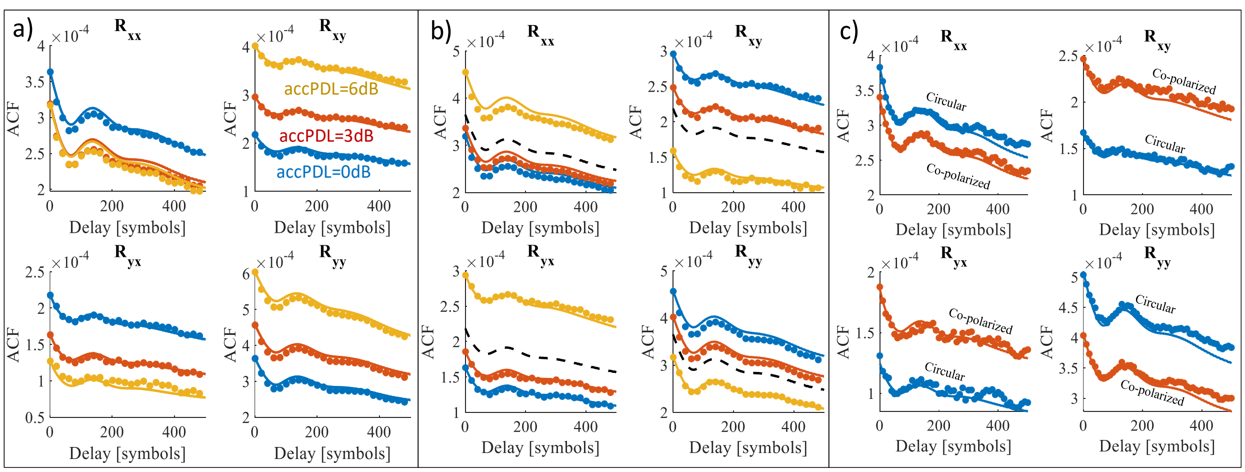

Fig. 2. Estimated ACFs for the four components of $\mathbf{R}_0^{(n)}$ for values of accumulated PDL (accPDL) of 0 dB, 3 dB and 6 dB (a), for different orientations of the PDL vectors with accumulated PDL of 3 dB (the black dashed curve refers to the case of no PDL (analytical results only) and colored curves refer to three different realizations of PDL vectors orientation) (b) and for different input SOPs of the IC, for the case of accumulated PDL of 3 dB (c)

In order to validate our results, we perform a set of SSFM simulations. In all cases, the simulated fiber link was composed of 15 spans of 100 km of G.652 fiber (α= 0:2 dB/km, β_2=-21,7 ps^2/km and γ=1.3W^{-1}km^{-1}). After each span, the fiber losses are compensated by a noiseless discrete amplifier, followed by a discrete PDL element. The orientation and strength of the PDL vectors of such components are chosen randomly to reach a target accumulated PDL value at the link end. The simulated system was composed of a channel of interest (COI) and a single interfering channel (IC), spaced 150 GHz apart. Both channels carry polarization multiplexed 16-QAM constellation, with a symbol rate of 68.7 GBaud. The launch power of the IC was 5 dBm, whereas that of the COI was -10 dBm. This ensures that the effects of SPM will be negligible compared to XPM. As the goal of this section is to ascertain the validity of the model, no other noise sources were considered (ASE, laser phase noise, etc.). At the receiver, the signal is detected and all linear transmission impairments (chromatic dispersion, PDL) are ideally compensated using static equalization.

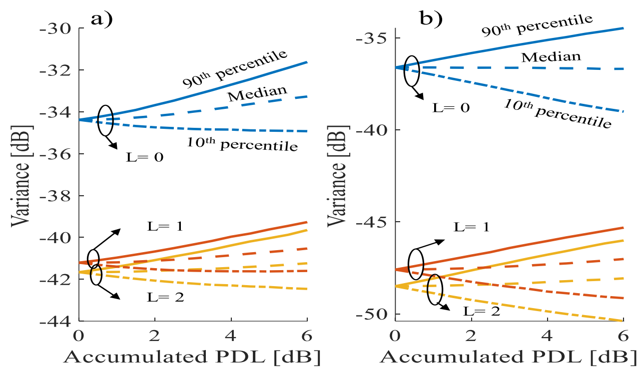

Fig. 3. Statics of the variances for different values of accumulated PDL and for ISI orders L=0, 1, 2, for R_{xx} and R_{yy} components (a) and for R_{xy} and R_{yx} components (b).

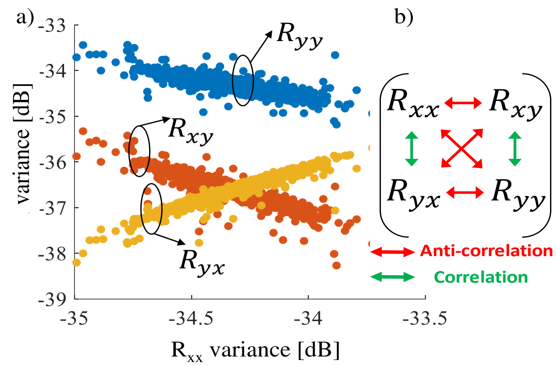

Fig. 4. Variances of R_{xy}, R_{yx} and R_{yy} vs. the variance of R_{xx} for L=0 and with accumulated PDL of 1dB (a), correlation relationship between the different matrix components (b)

For each simulation case, we estimated the auto-correlation functions (ACF) of each of the four components of the ISI matrices using the method described in [8]. These measured ACFs were then compared to the analytical results of the previous section. In all cases, the solid markers correspond to SSFM results and the lines to analytical results. Figure 2 (a) shows the simulation and analytical ACF for different values of total PDL. In this case the orientation of the PDL vectors was kept constant, and only their magnitude was changed to obtained an accumulated PDL of 0 dB (no PDL), 3dB and 6 dB. In all cases, the input SOP of the COI and IC are co-aligned. For the 0-th order ISI matrix – corresponding to phase and polarization noise (PPRN) – the influence of PDL is very significant. In the extreme case the phase noise affecting the two polarization channels is different by a factor of two (these are the R_{xx} and R_{yy} components). Polarization rotation noise (R_{xy} and R_{yx} components) also becomes more pronounced and may even become more significant than the phase noise. The effect of PDL is more subtle for higher order ISI matrices ($|L| > 0$), but is still present. Figure 2(b) shows the effect of varying only the orientation of PDL vectors when the magnitude of total PDL was kept constant at 3 dB. The SOP was also kept constant and identical for both channels. Both the phase and polarization noises can become either higher or lower than the reference case of no PDL, depending on the exact realization of PDL vectors was changed. Figure 2(c) shows the effect of the IC's input SOP. In this scenario, the PDL vectors were kept constant with an accumulated PDL level of 3 dB, and only the IC's SOP was changed. Two cases are shown: one where the COI and IC are co-polarized and one where the IC is rotated to circular polarization in the COI's frame of reference. Such a situation may naturally occur if, for example, the transmitters of COI and IC are spaced few meters apart and are combined through different input fibers. The input SOP can significantly affect PPRN (L= 0). However, for higher order ISI coefficient ($|L| > 0$), we found that the SOP has very little influence.

The main importance of the analytical model is that it allows to quickly explore different PDL settings, and investigates their influence on NLIN statistics. To demonstrate what type of analyses are possible, we generated 12000 different realizations of PDL vectors, and estimated the NLIN statistics for each case. Figure 3 shows the effect of the total accumulated PDL on the variance of ISI coefficients. As PDL is itself a stochastic process that changes very slowly compared to the symbol rate, it can either increase or decrease the NLIN noise power affecting each one of the polarizations. For example, the phase and polarization (L=0) noise variance in a system with 6 dB of accumulated PDL can be 3 dB larger than that of a system with no PDL. Similar behavior is observed for higher order ISI coefficients ($|L| > 0$). It should be noted that these results were obtained for co-aligned SOP for the COI and IC. If the SOP was also rotated randomly, it is expected that noise power will shift randomly between the on-diagonal elements and the of-diagonal elements. Fig 4 shows the relationships between the variances of the ISI matrix components, as the values of the PDL vectors are changed for an accumulated PDL of 1dB. If the PDL state causes the phase noise of polarization x to be high, then the phase noise of polarization y will be low, as the variances of R_{xx} and R_{yy} are anti-correlated. However, the polarization rotation noise affecting the polarization y will also increase, as the variances of R_{xx} and R_{yx} are positively-correlated. It should also be noted that the same behavior was observed for higher order ISI matrices as well ($|L| > 0$), and for every value of accumulated PDL.

5. Conclusion

We showed that in optical links affected by PDL, the time-varying ISI model for the XPM induced NLIN still holds, with the only difference is changing the statistical properties of the ISI coefficients. The model provides full second-order statistics of NLIN and enables to investigate a wide variety of PDL scenarios with low computational cost.

6. References

[1] A. Carena et al., Opt. Express, **22** (13), pp. 16335-16362, 2014
[2] R. Dar et al., Opt. Express, **21** (22), pp. 25685-25699, 2013.
[3] O. Golani et al., J. Lightw. Technol., **34** (14), pp. 3482-3489, 2016.
[4] R. Dar et al., J. Lightw. Technol., **35** (4), pp. 903–930, 2017.
[5] O. Golani et al., J. Lightw. Technol., **37** (9), pp. 1885-1892, 2019.
[6] D. Dahan et al., J. Lightw. Technol., **40** (8), pp. 2441-2455, 2022.
[7] P. Serena et al., J. Lightw. Technol., **38** (20), pp. 5685-5694, 2020.
[8] O. Golani et al., Optics Lett., **43** (5), pp. 1123-1126, 2018.